Reports of the Department of Mathematical Information Technology
Series B. Scientific Computing
No. B 1/2002

Fast Direct Solution of the Helmholtz Equation with a Perfectly Matched Layer/an Absorbing Boundary Condition

Erkki Heikkola Tuomo Rossi
Jari Toivanen

University of Jyväskylä 2002

Reports of the Department of Mathematical Information Technology
Series B. Scientific Computing

Editor Timo Tiihonen

Reports of the Department of Mathematical Information Technology
Series B. Scientific Computing
No. B 1/2002

Fast Direct Solution of the Helmholtz Equation with a Perfectly Matched Layer/an Absorbing Boundary Condition

Erkki Heikkola Tuomo Rossi
Jari Toivanen

University of Jyväskylä
Department of Mathematical Information Technology
P.O. Box 35 (Agora)
FIN–40351 Jyväskylä
FINLAND
fax +358 14 260 2731
http://www.mit.jyu.fi/

ISBN 951-39-1150-0
ISSN 1456-436X

Fast Direct Solution of the Helmholtz Equation with a Perfectly Matched Layer/an Absorbing Boundary Condition [*]

Erkki Heikkola, Tuomo Rossi, and Jari Toivanen
Department of Mathematical Information Technology
University of Jyväskylä, P.O. Box 35 (Agora)
FIN-40351 Jyväskylä, Finland
E-mail: emsh@mit.jyu.fi

Abstract

We consider efficient numerical solution of the Helmholtz equation in a rectangular domain with a perfectly matched layer (PML) or an absorbing boundary condition. Standard bilinear (trilinear) finite element discretization on an orthogonal mesh leads to a separable system of linear equations for which we describe a cyclic reduction type fast direct solver. We present numerical studies to estimate the reflection of waves by an absorbing boundary and a PML, and we optimize certain parameters of the layer to minimize the reflection.

Keywords: Helmholtz equation, perfectly matched layer, absorbing boundary conditions, finite element discretization, fast direct solver.

1 Introduction

We consider efficient numerical solution of the Helmholtz equation

$$-\Delta u - \omega^2 u = f, \quad \text{in } \mathbb{R}^d, \tag{1}$$

$$\lim_{r\to\infty} r^{(d-1)/2}\left(\frac{\partial u}{\partial r} - i\omega u\right) = 0, \tag{2}$$

with $d \geq 2$, which describes the linear propagation of time-harmonic acoustic waves. The Sommerfeld radiation condition (2) states that the solution u is outgoing at infinity. The finite element solution of this problem requires the unbounded domain to be truncated at a finite distance, and it becomes necessary to approximate the radiation condition at the truncation boundary. There are several different techniques to reduce spurious reflections caused by this artificial boundary such as local absorbing boundary conditions [9, 13], the exact nonlocal boundary condition [20, 24], and infinite elements [11].

The idea of the perfectly matched layer (PML) approach is to bound the domain by a finite layer of absorbing medium instead of a boundary. It is possible to construct a layer in which the

[*] This research was supported by the Academy of Finland, grant numbers 43066, 49006 and 66407.

magnitude of an incident wave of any frequency or angle of incidence is decreased exponentially with distance into the layer, thereby leading to low reflection. This approach was first proposed by Bérenger for the two-dimensional time-dependent Maxwell equations [4] and later extended to the three-dimensional case [5].

Research work on the PML-approach has mainly concentrated on computational electromagnetics, but similar techniques have proved to be useful also in computational acoustics [18, 25, 29]. The finite element solution of the Helmholtz equation with a PML has been studied recently in [14]. The application of the PML method to acoustic scattering is analyzed mathematically in [23]. It is proved that the resulting boundary value problem is uniquely solvable for all wave numbers and that its solution converges exponentially to the solution of the original problem when the thickness of the layer is increased.

In this work, we solve the Helmholtz equation in cartesian coordinates with a rectangular PML or absorbing boundary surrounding the computational domain (for PML in curvilinear coordinates, see [8]). The finite element discretization of the equations is performed with standard bilinear (trilinear) elements. The approximation of oscillatory functions by piecewise bilinear functions can be shown to be quasioptimal beyond the minimum resolution limit $\omega h = \pi/2$ [19]. However, quasioptimal error estimates for the finite element solution have been obtained only with the assumption that the quantity $\omega^2 h$ is sufficiently small. The boundedness of ωh, which corresponds to a certain number of nodes per wavelength, leads only to a suboptimal error estimate [12, 19]. In addition to the interpolation error, the L^2-norm of which is $\mathcal{O}(\omega^2 h^2)$, the error in the Galerkin finite element approximation involves also a pollution term of order $\omega^3 h^2$.

There are efficient direct solution methods for elliptic finite element equations in rectangular domains [28]. We describe the application of a specific cyclic reduction type fast direct method, called the PSCR-method, to the solution of the Helmholtz equation [26, 27, 30] and demonstrate its computational efficiency. This method can be used in similar manner both in the cases of a PML and a local absorbing boundary condition.

Fast direct solvers for elliptic equations in rectangular domains can be used as efficient preconditioners in the iterative solution of problems in more general domains [6]. There are various different methods, which are based on an equivalent formulation of the original problem to allow preconditioning with fast direct methods. Such techniques are referred to as fictitious domain, domain imbedding, or capacitance matrix methods, and they have been successfully applied also to acoustic scattering problems (see, for example, [10, 15, 16, 17]).

We study the reflection caused by the PML and the absorbing boundary on discrete level. We optimize certain parameters of the PML in different ways to minimize the reflection. These studies lead us to a convenient method to choose the parameters for the layer. The optimization of the PML has previously been considered in [7].

The rest of the paper is organized as follows: In Section 2, we formulate the Helmholtz equation with a PML or with an absorbing boundary condition and present the finite element discretization. The PSCR-method for the direct solution of the discrete equations is considered in Section 3. Our goal is to describe the method in a way to facilitate its practical implementation. In Section 4, we derive a formula of the reflection coefficient for a plane wave. The numerical experiments are reported in Section 5, and based on the results we draw some conclusions.

2 Formulation and discretization

We consider the variable-coefficient Helmholtz equation

$$-\nabla \cdot (\mathbf{A}\nabla u) - \omega^2 \gamma u = f, \qquad \text{in } \Pi, \tag{3}$$

$$\mathcal{B}\, u = 0, \qquad \text{on } \partial\Pi, \tag{4}$$

in the d-dimensional rectangular domain Π given by

$$\Pi = \prod_{k=1}^{d} [\check{x}_k, \hat{x}_k]. \tag{5}$$

Here, we have the diagonal matrix $\mathbf{A}(x)$

$$\mathbf{A}(x) = \operatorname*{diag}_{k=1,\ldots,d} \left\{ \frac{\gamma(x)}{\gamma_k^2(x_k)} \right\}, \quad \gamma(x) = \prod_{k=1}^{d} \gamma_k(x_k), \tag{6}$$

where the functions γ_k are of the form

$$\gamma_k(x_k) = 1 + \frac{i\,\sigma_k(x_k)}{\omega}. \tag{7}$$

The functions $\sigma_k(x_k)$ given by

$$\sigma_k(x_k) = \begin{cases} \sigma_0 \left(\frac{\check{x}_k + \delta - x_k}{\delta}\right)^p, & x_k < \check{x}_k + \delta, \\ 0, & \check{x}_k + \delta \le x_k \le \hat{x}_k - \delta, \\ \sigma_0 \left(\frac{x_k + \delta - \hat{x}_k}{\delta}\right)^p, & x_k > \hat{x}_k - \delta, \end{cases} \tag{8}$$

where δ, σ_0 and p are nonnegative constants.

We denote the outward normal to the boundary $\partial\Pi$ by $\mathbf{n}$ and a tangential direction by $\mathbf{s}$. The operator $\mathcal{B}$ defines the boundary condition on $\partial\Pi$, and with $\delta > 0$ we use either the Dirichlet or the Neumann boundary conditions given by $\mathcal{B}\, u = u$ and $\mathcal{B}\, u = \nabla u \cdot \mathbf{n}$, respectively. In these cases, equation (3) corresponds to the Helmholtz equation with a PML the parameter δ being the thickness of the layer. Also some other type of boundary conditions, such as an absorbing boundary condition, have been used on the outer boundary (see, for example, [7]). However, results suggest that the condition on the outer boundary does not have a significant effect on the accuracy.

If $\delta = 0$, the matrix $\mathbf{A}$ reduces to the identity matrix, and there is no absorbing layer. In this case, we impose either a first-order or a second-order local absorbing boundary condition on $\partial\Pi$. The first-order condition is given by $\mathcal{B}\, u = \nabla u \cdot \mathbf{n} - i\omega u$. For notational simplicity we present the second-order absorbing boundary condition only for the two-dimensional case, but it can be generalized in a straightforward manner to the d-dimensional case [2] (see also [15]). This condition involves the equation

$$\nabla u \cdot \mathbf{n} - i\omega u - \frac{i}{2\omega} \nabla \left(\nabla u \cdot \mathbf{s}\right) \cdot \mathbf{s} = 0 \tag{9}$$

on the faces of $\partial\Pi$ together with the equation $\nabla u \cdot \mathbf{s} = i\omega\frac{3}{2}u$ in the corners, denoted by C, of $\partial\Pi$.

For the weak formulation of the equation (3), we introduce the function spaces $V^D = H^1_0(\Pi)$, $V^N = V^F = H^1(\Pi)$, and $V^S = \{v \in V^N : v|_{\partial\Pi} \in H^1(\partial\Pi)\}$ corresponding to the four different boundary conditions. The Dirichlet and Neumann conditions lead to the sesquilinear form

$$a_D(u,v) = a_N(u,v) = \int_\Pi \big(\mathbf{A}\nabla u \cdot \nabla \bar{v} - \omega^2 \gamma u \bar{v}\big)\, dx, \tag{10}$$

while the absorbing boundary conditions correspond to the forms

$$a_F(u,v) = \int_\Pi \big(\nabla u \cdot \nabla \bar{v} - \omega^2 u \bar{v}\big)\, dx - i\omega \int_{\partial\Pi} u\bar{v}\, ds \quad \text{and} \tag{11}$$

$$a_S(u,v) = a_F(u,v) + \frac{i}{2\omega}\int_{\partial\Pi} \nabla u \cdot \mathbf{s}\, \nabla \bar{v} \cdot \mathbf{s}\, ds - \frac{3}{4}\sum_{x\in C} u(x)\bar{v}(x). \tag{12}$$

Now, the weak formulation of (3) can be represented in the following general form: Find $u \in V^m$ such that

$$a_m(u,v) = \int_\Pi f\bar{v}\, dx \quad \forall v \in V^m, \tag{13}$$

with $m = D, N, F$, or S.

The problem (13) is discretized by using bilinear (trilinear) finite elements on an orthogonal mesh. The mesh points in the x_k-direction are denoted by $x_{k,l}$, $l = 1, \ldots, n_k$, such that $x_{k,1} = \check{x}_k$ and $x_{k,n_k} = \hat{x}_k$. Such a discretization leads to a system of linear equations $\mathbf{K}\mathbf{u} = \mathbf{f}$, where the matrix $\mathbf{K}$ has a separable tensor product form, that is, by a suitable renumbering of the mesh nodes it can be represented in the form

$$\mathbf{K} = \big(\mathbf{A}^m_1 - \omega^2 \mathbf{M}^m_1\big) \otimes \mathbf{M}^m_2 + \mathbf{M}^m_1 \otimes \mathbf{A}^m_2, \quad m = D, N, F, S. \tag{14}$$

In the three-dimensional case, we obtain analogously the form

$$\mathbf{K} = \big(\mathbf{A}^m_1 - \omega^2 \mathbf{M}^m_1\big) \otimes \mathbf{M}^m_2 \otimes \mathbf{M}^m_3 + \mathbf{M}^m_1 \otimes \mathbf{A}^m_2 \otimes \mathbf{M}^m_3 + \mathbf{M}^m_1 \otimes \mathbf{M}^m_2 \otimes \mathbf{A}^m_3. \tag{15}$$

We calculate the entries of the matrices $\mathbf{A}^m_k$ and $\mathbf{M}^m_k$ by numerical quadrature, and we denote by q_j and w_j, $j = 1, \ldots, Q$, the quadrature points and the associated weight coefficients for a one-dimensional quadrature on the interval $[0,1]$. Furthermore, we introduce the notations $h_{k,l} = x_{k,l+1} - x_{k,l}$ and $\gamma_{k,l,j} = \gamma_k(x_{k,l} + q_j h_{k,l})h_{k,l}$. We remind that in the case $\delta = 0$ we have $\gamma_{k,l,j} = h_{k,l}$.

Then, the matrices $\mathbf{A}^D_k \in \mathbb{C}^{(n_k-2)\times(n_k-2)}$ in (14) and (15) are given by

$$\mathbf{A}^D_k = \begin{pmatrix} b_{k,2} & a_{k,2} & & \\ a_{k,2} & b_{k,3} & \ddots & \\ & \ddots & \ddots & a_{k,n_k-2} \\ & & a_{k,n_k-2} & b_{k,n_k-1} \end{pmatrix}, \tag{16}$$

where

$$b_{k,l} = \sum_{j=1}^{Q} w_j \left(\frac{1}{\gamma_{k,l-1,j}} + \frac{1}{\gamma_{k,l,j}}\right), \qquad l = 2, \ldots, n_k - 1, \tag{17}$$

$$a_{k,l} = -\sum_{j=1}^{Q} w_j \frac{1}{\gamma_{k,l,j}}, \qquad l = 1, \ldots, n_k - 1. \tag{18}$$

The matrices $\mathbf{A}_k^m \in \mathbb{C}^{n_k \times n_k}$ corresponding to the other three boundary conditions ($m = N, F, S$) are of the form

$$\mathbf{A}_k^m = \begin{pmatrix} b_{k,1}^m & \mathbf{a}_{k,1}^T & \\ \mathbf{a}_{k,1} & \mathbf{A}_k^D & \mathbf{a}_{k,n_k-1} \\ & \mathbf{a}_{k,n_k-1}^T & b_{k,n_k}^m \end{pmatrix}, \quad \mathbf{a}_{k,1} = \begin{pmatrix} a_{k,1} \\ 0 \\ \vdots \\ 0 \end{pmatrix}, \quad \mathbf{a}_{k,n_k-1} = \begin{pmatrix} 0 \\ \vdots \\ 0 \\ a_{k,n_k-1} \end{pmatrix}, \tag{19}$$

where entries $a_{k,l}$ are given by equation (18). The entries $b_{k,1}^m$ and b_{k,n_k}^m depend on the boundary condition such that

$$b_{k,1}^N = \sum_{j=1}^{Q} w_j \frac{1}{\gamma_{k,1,j}}, \qquad b_{k,n_k}^N = \sum_{j=1}^{Q} w_j \frac{1}{\gamma_{k,n_k-1,j}}, \tag{20}$$

$$b_{k,l}^F = b_{k,l}^N - i\omega, \qquad b_{k,l}^S = b_{k,l}^N - \frac{i\omega}{2}, \qquad l = 1, n_k. \tag{21}$$

The matrices $\mathbf{M}_k^D \in \mathbb{C}^{(n_k-2)\times(n_k-2)}$ are given by

$$\mathbf{M}_k^D = \begin{pmatrix} d_{k,2} & c_{k,2} & & \\ c_{k,2} & d_{k,3} & \ddots & \\ & \ddots & \ddots & c_{k,n_k-2} \\ & & c_{k,n_k-2} & d_{k,n_k-1} \end{pmatrix}, \tag{22}$$

where

$$d_{k,l} = \sum_{j=1}^{Q} w_j \left(\gamma_{k,l-1,j}(1-q_j)^2 + \gamma_{k,l,j}\, q_j^2\right), \qquad l = 2, \ldots, n_k - 1, \tag{23}$$

$$c_{k,l} = \sum_{j=1}^{Q} w_j\, \gamma_{k,l,j}(1-q_j)q_j, \qquad l = 1, \ldots, n_k - 1. \tag{24}$$

The matrices $\mathbf{M}_k^m \in \mathbb{C}^{n_k \times n_k}$ corresponding to the other boundary conditions are of the form

$$\mathbf{M}_k^m = \begin{pmatrix} d_{k,1}^m & \mathbf{c}_{k,1}^T & \\ \mathbf{c}_{k,1} & \mathbf{M}_k^D & \mathbf{c}_{k,n_k-1} \\ & \mathbf{c}_{k,n_k-1}^T & d_{k,n_k}^m \end{pmatrix}, \quad \mathbf{c}_{k,1} = \begin{pmatrix} c_{k,1} \\ 0 \\ \vdots \\ 0 \end{pmatrix}, \quad \mathbf{c}_{k,n_k-1} = \begin{pmatrix} 0 \\ \vdots \\ 0 \\ c_{k,n_k-1} \end{pmatrix}, \tag{25}$$

where entries $c_{k,l}$ are given by equation (24). The entries $d_{k,1}^m$ and d_{k,n_k-1}^m depend on the boundary condition such that

$$d_{k,1}^N = \sum_{j=1}^{Q} w_j \gamma_{k,1,j} q_j^2, \qquad d_{k,n_k}^N = \sum_{j=1}^{Q} w_j \gamma_{k,n_k-1,j}(1-q_j)^2, \tag{26}$$

$$d_{k,l}^F = d_{k,l}^N, \qquad d_{k,l}^S = d_{k,l}^N + \frac{i}{2\omega}, \qquad l = 1, n_k. \tag{27}$$

3 Fast direct solution

We apply the partial solution variant of the cyclic reduction (PSCR) algorithm to solve linear systems with the separable matrix $\mathbf{K}$. This method was introduced in [30] and further developed in [21, 26, 27]. It is a cyclic reduction type algorithm which uses the partial solution method [3, 22] instead of matrix polynomials. Here, we describe the implementation of the PSCR-method in a general radix–r framework, while the parallel implementation of the radix–4 variant is described in [27]. Furthermore, we show that it requires $\mathcal{O}(n_1 n_2 \log n_1)$ operations for two-dimensional problems and $\mathcal{O}(n_1 n_2 n_3 \log n_1 \log n_2)$ operations for three-dimensional problems.

3.1 The partial solution variant of the cyclic reduction

The algorithm operates on $m = \lceil \log_r(n_1 + 1) \rceil$ levels with r^{k-1} subproblems on the kth level. These problems are defined by dividing the mesh nodes into r^{k-1} groups in the x_1-direction such that the dividing mesh coordinates are $x_{1,l_{k,j}}$, where the indices $l_{k,j}$ are given by

$$l_{k,j} = \begin{cases} 0, & j = 1, \\ \lfloor (j-1)n_1/r^{k-1} + 1 \rfloor, & 1 < j \le r^{k-1} + 1. \end{cases} \tag{28}$$

Then, the jth subproblem corresponds to the index set

$$S_{k,j} = \{l_{k,j} + 1, \ldots, l_{k,j+1} - 1\} \tag{29}$$

in the x_1-direction. We note that on the level $k = m$, some of the subproblems might vanish.

In order to describe the algorithm, we first introduce the following index sets:

$$P_{k,j} = \{l_{k+1,r(j-1)+2}, l_{k+1,r(j-1)+3}, \ldots, l_{k+1,r(j-1)+r}\}, \tag{30}$$

$$R_{k,j} = \begin{cases} \{l_{k,j+1}\}, & j = 1, \\ \{l_{k,j}, l_{k,j+1}\}, & 1 < j < r^{k-1}, \\ \{l_{k,j}\}, & j = r^{k-1}, \end{cases} \tag{31}$$

$$T_{k,j} = \begin{cases} \{l_{k,j+1} - 1\}, & j = 1, \\ \{l_{k,j} + 1, l_{k,j+1} - 1\}, & 1 < j < r^{k-1}, \\ \{l_{k,j} + 1\}, & j = r^{k-1}, \end{cases} \tag{32}$$

for $k = 1, \ldots, m$ and $j = 1, \ldots, r^{k-1}$. Furthermore, we define the renumbered sets

$$\hat{P}_{k,j} = \bigcup_{t \in P_{k,j}} \{t - l_{k,j}\} \qquad \text{and} \qquad \hat{T}_{k,j} = \bigcup_{t \in T_{k,j}} \{t - l_{k,j}\}. \tag{33}$$

We use a special notation for submatrices and subvectors. For this purpose, let the members of the index sets P and R be $p_1, \ldots, p_{n_p}$ and $r_1, \ldots, r_{n_r}$ in ascending order and with the possible multiple appearances removed, respectively. Then, the subvector $\mathbf{f}(P)$ is defined to be

$$\mathbf{f}(P) = \begin{pmatrix} \mathbf{f}(p_1) \\ \mathbf{f}(p_2) \\ \vdots \\ \mathbf{f}(p_{n_p}) \end{pmatrix}, \quad \text{where} \quad \mathbf{f}(p) = \begin{pmatrix} \mathbf{f}_{(p-1)n+1} \\ \mathbf{f}_{(p-1)n+2} \\ \vdots \\ \mathbf{f}_{pn} \end{pmatrix}. \tag{34}$$

Here, n is n_2 for two-dimensional problems and $n_2 n_3$ for three-dimensional problems. Similarly, we define the submatrix

$$\mathbf{K}(P,T) = \begin{pmatrix} \mathbf{K}(p_1,t_1) & \mathbf{K}(p_1,t_2) & \cdots & \mathbf{K}(p_1,t_{n_t}) \\ \mathbf{K}(p_2,t_1) & \mathbf{K}(p_2,t_2) & \cdots & \mathbf{K}(p_2,t_{n_t}) \\ \vdots & \vdots & \ddots & \vdots \\ \mathbf{K}(p_{n_p},t_1) & \mathbf{K}(p_{n_p},t_2) & \cdots & \mathbf{K}(p_{n_p},t_{n_t}) \end{pmatrix}, \tag{35}$$

where

$$\mathbf{K}(p,t) = \begin{pmatrix} \mathbf{K}_{(p-1)n+1,(t-1)n+1} & \mathbf{K}_{(p-1)n+1,(t-1)n+2} & \cdots & \mathbf{K}_{(p-1)n+1,tn} \\ \mathbf{K}_{(p-1)n+2,(t-1)n+1} & \mathbf{K}_{(p-1)n+2,(t-1)n+2} & \cdots & \mathbf{K}_{(p-1)n+2,tn} \\ \vdots & \vdots & \ddots & \vdots \\ \mathbf{K}_{pn,(t-1)n+1} & \mathbf{K}_{pn,(t-1)n+2} & \cdots & \mathbf{K}_{pn,tn} \end{pmatrix}. \tag{36}$$

Now, we can present the PSCR-algorithm as follows:

Algorithm 1 *PSCR-method for computing* $\mathbf{f} = \mathbf{K}^{-1}\mathbf{f}$.

```
**do** $k = m, 2, -1$
   **do** $j = 1, r^{k-1}$
      **if** $l_{k,j+1} - l_{k,j} > 1$ **then**
         $\mathbf{f}(R_{k,j}) = \mathbf{f}(R_{k,j}) - \mathbf{K}(R_{k,j}, T_{k,j})(\mathbf{K}(S_{k,j}, S_{k,j}))^{-1}(\hat{T}_{k,j}, \hat{P}_{k,j})\mathbf{f}(P_{k,j})$
      **end if**
   **end do**
**end do**
$\mathbf{f}(P_{1,1}) = \mathbf{K}^{-1}(P_{1,1}, P_{1,1})\mathbf{f}(P_{1,1})$
**do** $k = 2, m$
   **do** $j = 1, r^{k-1}$
      **if** $l_{k,j+1} - l_{k,j} > 1$ **then**
         $\mathbf{f}(P_{k,j}) = (\mathbf{K}(S_{k,j}, S_{k,j}))^{-1}(\hat{P}_{k,j}, \hat{P}_{k,j} \cup \hat{T}_{k,j})$
                    $(\mathbf{I}(P_{k,j} \cup T_{k,j}, P_{k,j})\mathbf{f}(P_{k,j})$
                     $- \mathbf{I}(P_{k,j} \cup T_{k,j}, T_{k,j})\mathbf{K}(T_{k,j}, R_{k,j})\mathbf{f}(R_{k,j}))$
      **end if**
   **end do**
**end do**.
```

The identity matrix **I** in Algorithm 1 has the same size as the matrix $\mathbf{K}$. The submatrices of **I** are used to assemble vectors to a suitable structure for subproblems.

The vectors multiplied by the inverse matrices in Algorithm 1 have only a few nonzero components and only a sparse subset of the components of the resulting vectors are required. Due to this sparsity of the arising subproblems, it is shown in Section 3.2 that the solution of the jth subproblem on the kth level requires $\mathcal{O}((l_{k,j+1} - l_{k,j})n_2)$ operations for two-dimensional problems and $\mathcal{O}((l_{k,j+1} - l_{k,j})n_2 n_3 \log n_2)$ operations for three-dimensional problems. By summing these over all $\mathcal{O}(\log n_1)$ levels, we obtain the computational complexities given in the beginning of this section.

3.2 Partial solution method

The partial solution method for the direct solution of linear systems corresponding to elliptic equations in rectangular domains was introduced in [3, 22]. The method is a special implementation of the classical method of separation of variables, and its efficiency is based on the assumptions that only a sparse set of the solution components of the linear system is required and that the right-hand side vector has only a few nonzero components. Then, the partial solution procedure is obtained directly from the method of separation variables by neglecting arithmetical operations with the zero components. In the following, we consider the multiplication by $\mathbf{K}^{-1}(P, T)$. All the other subproblems in Algorithm 1 have a similar structure and, thus, they can be solved in the same way.

The method of separation of variables involves solution of the generalized eigenvalue problem

$$\mathbf{A}_1^m \mathbf{W} = \mathbf{M}_1^m \mathbf{W} \Lambda, \tag{37}$$

where the matrix $\mathbf{W}$ contains the eigenvectors as its columns, and the diagonal matrix Λ contains the eigenvalues $\lambda_1, \ldots, \lambda_{n_1}$. It is necessary for the applicability of the method that the eigenvectors form a basis for the space $\mathbb{C}^{n_1}$ and satisfy the condition $\mathbf{W}^T \mathbf{M}_1^m \mathbf{W} = \mathbf{I}$. The eigenvalue problem (37) is solved once in the initialization stage of the solver. Now, it is straightforward to see that the inverse of $\mathbf{K}$ in (14) (two-dimensional problem) is

$$\mathbf{K}^{-1} = (\mathbf{W} \otimes \mathbf{I})((\Lambda - \omega^2 \mathbf{I}) \otimes \mathbf{M}_2^m + \mathbf{I} \otimes \mathbf{A}_2^m)^{-1}(\mathbf{W}^T \otimes \mathbf{I}) \tag{38}$$

and the inverse of $\mathbf{K}$ in (15) (three-dimensional problem) is

$$\mathbf{K}^{-1} = (\mathbf{W} \otimes \mathbf{I})(((\Lambda - \omega^2 \mathbf{I}) \otimes \mathbf{M}_2^m + \mathbf{I} \otimes \mathbf{A}_2^m) \otimes \mathbf{M}_3^m + \mathbf{M}_1 \otimes \mathbf{M}_2 \otimes \mathbf{A}_3)^{-1}(\mathbf{W}^T \otimes \mathbf{I}). \tag{39}$$

Note that FFT-transformation cannot be used to perform the multiplications with $\mathbf{W}$ and $\mathbf{W}^T$, since these matrices are not of suitable form.

By exploiting the special sparsity of problem, we obtain the following partial solution algorithm for two-dimensional problems.

Algorithm 2 *Partial solution method for computing* $\mathbf{v} = \mathbf{K}^{-1}(P, T)\mathbf{g}$.

```
$\mathbf{v} = \mathbf{0}$
**do** $k = 1, n_1$
    $\hat{\mathbf{g}} = (\mathbf{W}^T \otimes \mathbf{I})(\{k\}, T)\mathbf{g}$
    $\hat{\mathbf{v}} = ((\lambda_k - \omega^2)\mathbf{M}_2^m + \mathbf{A}_2^m)^{-1}\hat{\mathbf{g}}$
    $\mathbf{v} = \mathbf{v} + (\mathbf{W} \otimes \mathbf{I})(P, \{k\})\hat{\mathbf{v}}$
**end do**
```

In Algorithm 2, the computation of $\hat{\mathbf{g}}$ requires $\mathcal{O}(n_2 \# T)$ operations, where $\# T$ is the number of members in the set T. In our case $\# T = \mathcal{O}(1)$ and, thus, the cost is $\mathcal{O}(n_2)$ operations. The computation of $\hat{\mathbf{v}}$ requires the solution of a system of linear equations with the tridiagonal matrix $(\lambda_k - \omega^2)\mathbf{M}_2^m + \mathbf{A}_2^m$. Therefore, the cost is $\mathcal{O}(n_2)$ operations. Finally, the cost of computing $\mathbf{v}$ is $\mathcal{O}(n_2 \# P)$ operations, which is $\mathcal{O}(n_2)$ operations in our case. All these steps are performed n_1 times and, thus, one partial solution requires $\mathcal{O}(n_1 n_2)$ operations for two-dimensional problems.

For three-dimensional problems, the partial solution method has the same structure as Algorithm 2. In this case, the multiplications by $(\mathbf{W}^T \otimes \mathbf{I})(\{k\}, T)$ and $(\mathbf{W} \otimes \mathbf{I})(P, \{k\})$ require

$\mathcal{O}(n_2 n_3)$ operations when $\#T = \mathcal{O}(1)$ and $\#P = \mathcal{O}(1)$. Now, the matrix $((\Lambda - \omega^2 \mathbf{I}) \otimes \mathbf{M}_2^m + \mathbf{I} \otimes \mathbf{A}_2^m) \otimes \mathbf{M}_3^m + \mathbf{M}_1 \otimes \mathbf{M}_2 \otimes \mathbf{A}_3$ is block tridiagonal and the application of LU-decomposition is too expensive. Instead, we use the PSCR-method for two-dimensional problems to solve the corresponding linear systems. Thus, this step costs $\mathcal{O}(n_2 n_3 \log n_2)$ operations. By summing up the operation counts in the loop from 1 to n_1, we obtain that the cost of the solution of one partial solution problem for three-dimensional problems requires $\mathcal{O}(n_1 n_2 n_3 \log n_2)$ operations.

4 Reflection coefficient for perpendicular plane wave

For simplicity, we restrict our attention to a two-dimensional problem with a uniform mesh step size h. We consider a plane wave traveling to the positive x_1-direction and study its reflection by the right layer or the absorbing boundary. A similar analysis to the following one has been performed for discretized Maxwell equations with a PML in [7].

Let us assume that the solution of the Helmholtz equation is a finite element function which is independent on the x_2-coordinate. Then, the nodal values are given by $u(x_{1,j}, x_{2,l}) = v_j$, $j = 1, \ldots, n_1$, $l = 1, \ldots, n_2$, where v_j is the jth component of a vector $\mathbf{v} = (v_j)_{j=1}^{n_1}$. By substituting the nodal values to the linear system $\mathbf{K}\mathbf{u} = \mathbf{0}$, it follows easily from the rows corresponding to the nodes outside the upper and lower layers or boundaries that $\mathbf{v}$ satifies the equation

$$\left(\mathbf{A}_1^m - \omega^2 \mathbf{M}_1^m\right) \mathbf{v} = \mathbf{0}. \tag{40}$$

Let $x_{1,k-1}$ be the node one mesh step h left from the right layer or boundary. Furthermore, let the amplitude of the wave traveling right be one and the amplitude of the reflected wave be $|R|$. Thus, the nodal value at $x_{1,k-1}$ can be chosen to be

$$v_{k-1} = 1 + R. \tag{41}$$

The nodal value at $x_{1,k}$ can be solved using the value v_{k-1} and the equations in (40), which lead to

$$v_k = -\alpha v_{k-1}, \tag{42}$$

where

$$\alpha = (a_{1,k-1} - \omega^2 c_{1,k-1}) \mathbf{e}^T \left(\mathbf{K}_{1,k}^m\right)^{-1} \mathbf{e}. \tag{43}$$

Here, the matrix $\mathbf{K}_{1,k}^m$ is the submatrix of $\mathbf{A}_1^m - \omega^2 \mathbf{M}_1^m$ given by

$$\mathbf{K}_{1,k}^m = \left(\mathbf{A}_1^m - \omega^2 \mathbf{M}_1^m\right)_{j,l=k}^{n_1-1} \quad \text{or} \quad \mathbf{K}_{1,k}^m = \left(\mathbf{A}_1^m - \omega^2 \mathbf{M}_1^m\right)_{j,l=k}^{n_1} \tag{44}$$

for Dirichlet boundary value problems or problems with other boundary conditions, respectively, and the vector $\mathbf{e}$ is defined by $\mathbf{e}^T = (1 \ 0 \ \cdots \ 0)$.

For a plane wave traveling directly to left or right, it is easy to see that the first-order absorbing boundary condition and the second-order are identical on the left and right boundaries. In this case, the coefficient α is

$$\alpha = \frac{a_{1,n_1-1} - \omega^2 c_{1,n_1-1}}{b_{1,n_1}^F - \omega^2 d_{1,n_1}^F}. \tag{45}$$

Another special case is when Dirichlet boundary conditions are posed on $\partial\Pi$ and the exponent p in (8) is zero. Then, with the help of the result in Appendix A, we obtain

$$\alpha = \frac{a_{1,k-1} - \omega^2 c_{1,k-1}}{b_{1,k} - \omega^2 d_{1,k} - (a_{1,k} - \omega^2 c_{1,k})\beta}, \tag{46}$$

where

$$\beta = 2\frac{(\rho - \sqrt{\rho^2-4})^{n_1-k} - (\rho + \sqrt{\rho^2-4})^{n_1-k}}{(\rho - \sqrt{\rho^2-4})^{n_1-k+1} - (\rho + \sqrt{\rho^2-4})^{n_1-k+1}} \qquad \text{and} \qquad \rho = \frac{b_{1,k+1} - \omega^2 d_{1,k+1}}{a_{1,k} - \omega^2 c_{1,k}}. \tag{47}$$

Clearly, the denominators of α, β and ρ have to be nonzero.

On the other hand, we know that the solution has the form $v_j = e^{i\hat{\omega}(j-k+1)h} + Re^{-i\hat{\omega}(j-k+1)h}$ on the nodes outside the layers. Here, $\hat{\omega}$ is the discrete wave number taking into account the phase shift caused by the discretization [1] and it is given by

$$\hat{\omega} = \frac{1}{h}\arccos\left(-\frac{b_{1,k-1} - \omega^2 d_{1,k-1}}{2(a_{1,k-1} - \omega^2 c_{1,k-1})}\right). \tag{48}$$

Thus, the nodal value at $x_{1,k}$ is

$$v_k = e^{i\hat{\omega}h} + Re^{-i\hat{\omega}h}. \tag{49}$$

The reflection coefficient R can be solved from the equations (41), (42) and (49) to obtain

$$R = -\frac{1 + \alpha e^{-i\hat{\omega}h}}{1 + \alpha e^{i\hat{\omega}h}}. \tag{50}$$

5 Numerical experiments

We study numerically the reflection of waves caused by the PML and the artificial boundary $\partial\Pi$ with the second-order absorbing boundary condition. Our aim is to determine the appropriate thickness of the PML and the distance of the absorbing boundary in order to make the error caused by the reflection smaller than the discretization error. For these tests, the parameters σ_0 and p in (8) of the PML are optimized to minimize the reflection. We also study the efficiency of the fast direct solver. Most of the experiments are performed with two-dimensional problems, but we present also some results with three-dimensional problems. All the numerical experiments were performed in a J5600 HP workstation (PA-8600 CPU at 552MHz).

In the experiments, the computational domain is $\prod_{k=1}^{d}[-1-\delta, 1+\delta]$, that is, we have $\check{x}_k = -1-\delta$ and $\hat{x}_k = 1+\delta$ in (5). The wave number is chosen to be $\omega = 2\pi$, which corresponds to the wavelength $\lambda = 1$. The discretization meshes are uniform and with the same mesh step size h in all directions. Thus, using the notations of Section 2 we have $n_k = n$ and $x_{k,l} = -1-\delta+(l-1)h$, where $h = 2(1+\delta)/(n-1)$. We use the four point Gauss quadrature ($Q = 4$), which defines the points q_j and the weights w_j in Section 2.

The right-hand side vector $\mathbf{f}$ is chosen to be such that the component corresponding to the origin is equal to one and all the other are zero. Thus, the solution u is an approximation of the Green function g, which for two-dimensional problems, is $iH_0^{(1)}(\omega r)/4$ and, for three-dimensional problems, $e^{i\omega r}/(4\pi r)$. Here, $H_0^{(1)}$ is the Hankel function and r is the euclidean distance from the origin. The reflection and the discretization error are measured using the L^2-norm in the domain $D = \prod_{k=1}^{d}[-1,1] \setminus \prod_{k=1}^{d}[-1/2,1/2]$. See Figure 1 for an illustration of two-dimensional test problems.

We begin by optimizing the parameters σ_0 and p for the PML in two-dimensional problems. The optimization results indicate an easy way to choose σ_0 and p such that the reflection is reasonably low. In the tests, the number of nodes per wavelength (λ/h) obtains the values 8, 16, and 32, while the width of the absorbing layer is 8, 16, or 32 mesh steps h (δ/h).

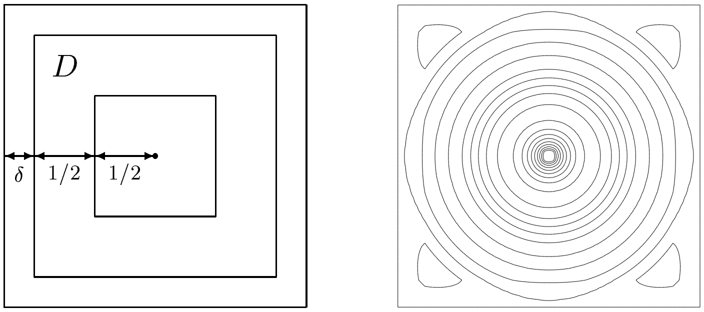

Figure 1: The two-dimensional test problem with notations and some isolines of a solution.

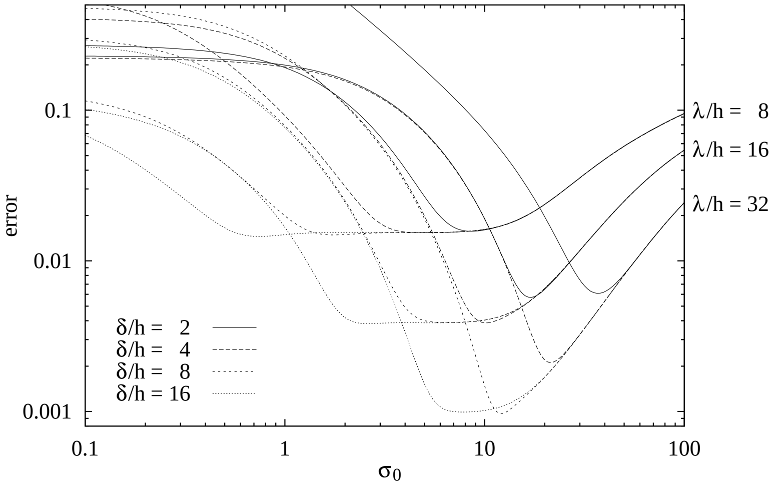

Figure 2: The L^2-norm of the error $u - g$ for different values of σ_0.

First, we choose the parameters in such a way that the error $||u - g||_{L^2(D)}$ is minimized, that is,

$$(\sigma_0, p) = \underset{(\sigma_0, p)}{\operatorname{argmin}} ||u - g||_{L^2(D)}. \tag{51}$$

After this we fix the exponent p to be zero which means that the σ function is constant in the PML. Figure 2 shows how the L^2-norm of the error behaves with respect to σ_0 in this case. It can be seen that for some layers the value of σ_0 must be chosen quite accurately in order to obtain a small error. We use the following two ways to choose the σ_0 parameter:

$$\sigma_0 = \underset{\sigma_0, p=0}{\operatorname{argmin}} ||u - g||_{L^2(D)} \qquad \text{and} \qquad \sigma_0 = \underset{\sigma_0, p=0}{\operatorname{argmin}} |R|. \tag{52}$$

The first one of (52) minimizes the L^2-norm of the error while the second one minimizes the modulus of the reflection coefficient R.

The results are given in Table 1 where the choice 1 corresponds to (51) and the choices 2 and 3 correspond to the left-hand side and the right-hand side of (52), respectively. The minimization (51) was performed by sampling 41 values for p in $[0, 4]$ and 301 values for σ_0 in $[0.1, 100]$ and, then, by choosing the one with the smallest error. Based on these results it can be concluded that by choosing $p = 0$ we obtain almost best possible accuracy. Furthermore, the minimization of $|R|$ gives a good way to choose σ_0 when $p = 0$. This one-dimensional minimization can be easily performed numerically.

The results in Table 1 give an idea how thick the layer should be in order to have the reflection error approximately equal to the discretization error. This comparison is more obvious

Table 1: The results of optimizing the parameters σ_0 and p in the PML.

		choice 1			choice 2		choice 3	
λ/h	δ/h	p	σ_0	error	σ_0	error	σ_0	error
8	2	0.5	10.96	0.01478	8.56	0.01572	7.62	0.01601
8	4	0.6	8.71	0.01514	4.83	0.01538	5.10	0.01538
8	8	1.7	4.47	0.01456	1.75	0.01486	2.97	0.01534
8	16	4.0	3.63	0.01431	4.59	0.01541	1.72	0.01545
16	2	0.0	16.98	0.00572	16.98	0.00572	15.18	0.00625
16	4	0.2	10.96	0.00376	10.17	0.00388	9.52	0.00394
16	8	3.1	19.05	0.00389	6.46	0.00390	6.18	0.00390
16	16	2.3	7.94	0.00383	2.59	0.00384	3.46	0.00388
32	2	0.0	37.15	0.00608	36.99	0.00608	33.70	0.00634
32	4	0.0	21.38	0.00211	21.38	0.00211	19.34	0.00232
32	8	0.1	12.59	0.00096	12.12	0.00097	11.58	0.00099
32	16	3.0	23.44	0.00098	7.85	0.00099	7.45	0.00099

from Figure 3, which shows how the errors $||u - g||_{L^2(D)}$ for the PML and the second-order absorbing boundary condition behave when the width δ is changed. For the PML, $p = 0$ and σ_0 is obtained by minimizing $|R|$. The errors for the two approaches are almost the same with small differences for small values of δ.

For exactly the same problems, the reflection coefficient R is plotted in Figure 4. The modulus of R oscillates for the PML while it is constant for the absorbing boundary conditions. For three-dimensional problems, the error is shown in Figure 5 with the parameters of the PML chosen in the same way as for the two-dimensional problems. It can be seen that the error behaves similarly for two-dimensional and three-dimensional problems.

In our last experiments, we study the efficiency of the fast direct solver. In the initialization stage, one-dimensional generalized eigenvalue problems have to be solved. For this purpose, we use the subroutine F02GJF from the NAG Fortran library. It is an implementation of the complex QZ algorithm, and it requires $\mathcal{O}(n^3)$ operations. This cost is greater than the cost of the actual solution method for two-dimensional problems but smaller than that for three-dimensional problems. For two-dimensional problems, CPU times for the initialization and the solution are given in Table 2. Similar timings for three-dimensional problems are given in Table 3. In these tables, the solution times behave quite expectedly with slightly faster growth than the estimates predict. This is probably due to some cache memory effects on CPU.

The tables clearly show that, for two-dimensional problems, the initialization is far more expensive than the actual solution, while for three-dimensional problems the situation is the opposite. Thus, the solver for eigenproblems should be replaced with a more efficient one at least for two-dimensional problems. The situation is balanced by the fact that the initialization needs to be performed only once, but often the fast direct solver is applied several times, for example, during an iterative solution procedure.

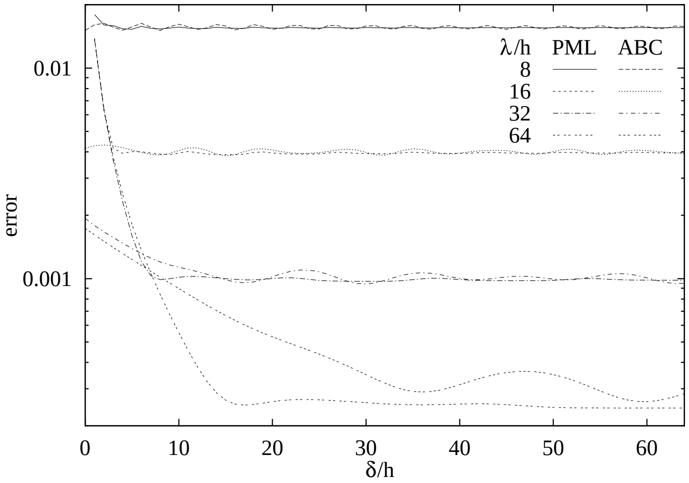

Figure 3: The L^2-norm of the error $u - g$ for different discretizations in the two-dimensional case.

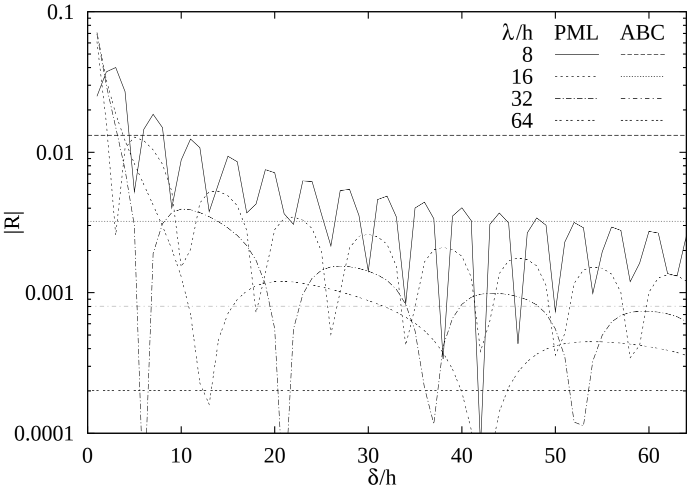

Figure 4: The modulus of the reflection coefficient for different discretizations.

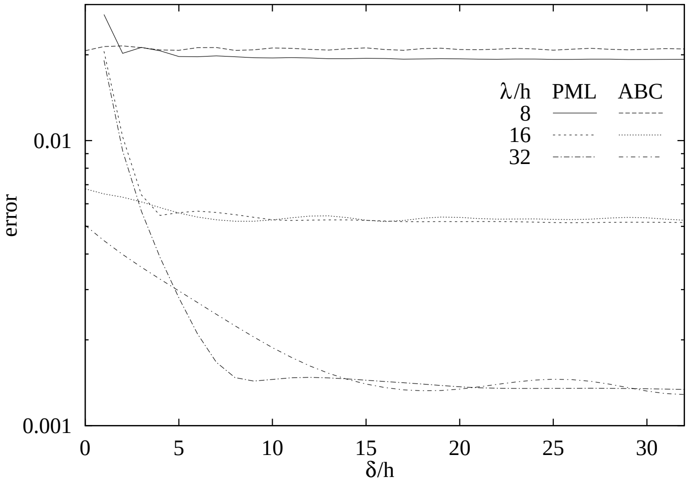

Figure 5: The L^2-norm of the error $u - g$ for different discretizations in the three-dimensional case.

Table 2: CPU times in seconds for two-dimensional problems.

n	65	129	257	513	1025
initialization	0.11	0.77	10.13	126.68	1490.87
solution	0.01	0.05	0.25	1.13	4.53

Table 3: CPU times in seconds for three-dimensional problems.

n	9	17	33	65	129	257
initialization	0.00	0.01	0.03	0.21	1.52	18.91
solution	0.01	0.03	0.37	3.33	46.87	419.14

6 CONCLUSIONS

We considered the numerical solution of the Helmholtz equation in a rectangular domain with a perfectly matched layer or an absorbing boundary condition. Suitable finite element discretization of this equation leads to a separable linear system for which we presented an efficient fast direct solution method, called the PSCR-method. We studied numerically the reflection of waves by the PML and the absorbing boundary. Results showed, for example, the appropriate thickness of the PML and the distance of the absorbing boundary to make the reflection error to be of the same order as the discretization error. We optimized the parameters of the PML to minimize reflection, which led us to a convenient method to choose these parameters to obtain reasonably low reflection.

A Diagonal entry for the inverse of a symmetric tridiagonal Toeplitz matrix

Let us derive a formula for the entry $(\mathbf{A}^{-1})_{n,n}$ of a tridiagonal $n \times n$ Toeplitz matrix $\mathbf{A}$ with the codiagonal elements being one. We denote a generic diagonal element by $\rho \in \mathbb{C}$. It is clear that the LU-decomposition $\mathbf{A} = \mathbf{L}\mathbf{U}$, when it exists, has bidiagonal factors $\mathbf{L}$ and $\mathbf{U}$ with $\mathbf{L}$ being a lower triangular matrix and $\mathbf{U}$ an upper triangular matrix. Furthermore, the diagonal entries of $\mathbf{U}$ can be chosen to be ones. Hence, the last diagonal entry of $\mathbf{A}^{-1}$ equals the inverse of the entry $\mathbf{L}_{n,n}$. In the following, we denote $l_k = \mathbf{L}_{k,k}$ for $k = 1, \dots, n$, and it is straightforward to see that these coefficients satisfy the recurrence relation

$$\begin{aligned} l_1 &= \rho, \\ l_k &= \frac{\rho\, l_{k-1} - 1}{l_{k-1}}, \quad \forall\, k = 2, \dots, n. \end{aligned} \tag{53}$$

We see by induction that $l_k = \frac{x_k}{y_k}$, where x_k and y_k can be computed by

$$\begin{aligned} \begin{pmatrix} x_1 \\ y_1 \end{pmatrix} &= \begin{pmatrix} \rho \\ 1 \end{pmatrix}, \\ \begin{pmatrix} x_k \\ y_k \end{pmatrix} &= \begin{pmatrix} \rho & -1 \\ 1 & 0 \end{pmatrix}^{k-1} \begin{pmatrix} x_1 \\ y_1 \end{pmatrix}, \quad \forall\, k = 2, \dots, n. \end{aligned} \tag{54}$$

Hence,

$$(A^{-1})_{n,n} = l_n^{-1} = \frac{y_n}{x_n}, \quad \text{where} \quad \begin{pmatrix} x_n \\ y_n \end{pmatrix} = \begin{pmatrix} \rho & -1 \\ 1 & 0 \end{pmatrix}^{n-1} \begin{pmatrix} \rho \\ 1 \end{pmatrix}. \tag{55}$$

We shall assume that $\rho \neq \pm 2$. Then, it follows that the matrix in (54) is similar to a diagonal matrix, and we have the decomposition

$$\begin{pmatrix} \rho & -1 \\ 1 & 0 \end{pmatrix}^k = \begin{pmatrix} \frac{\rho-\sqrt{\rho^2-4}}{2} & \frac{\rho+\sqrt{\rho^2-4}}{2} \\ 1 & 1 \end{pmatrix} \begin{pmatrix} \frac{\rho-\sqrt{\rho^2-4}}{2} & 0 \\ 0 & \frac{\rho+\sqrt{\rho^2-4}}{2} \end{pmatrix}^k \begin{pmatrix} \frac{\rho-\sqrt{\rho^2-4}}{2} & \frac{\rho+\sqrt{\rho^2-4}}{2} \\ 1 & 1 \end{pmatrix}^{-1}. \tag{56}$$

Using the decomposition (56) in (55), straightforward calculations lead to the formula

$$(A^{-1})_{n,n} = 2\frac{(\rho-\sqrt{\rho^2-4})^n - (\rho+\sqrt{\rho^2-4})^n}{(\rho-\sqrt{\rho^2-4})^{n+1} - (\rho+\sqrt{\rho^2-4})^{n+1}}. \tag{57}$$

Both the equation (53) and the above expression are well-defined when

$$(\rho-\sqrt{\rho^2-4})^k - (\rho+\sqrt{\rho^2-4})^k \neq 0 \quad \forall\, k = 1, \ldots, n+1. \tag{58}$$

After solving (58) for ρ, we obtain that ρ should not belong to the set

$$\bigcup_{k=1}^{n+1} \bigcup_{j=1}^{k+1} \left\{ 2\cos\left(\frac{(j-1)\pi}{k}\right) \right\}. \tag{59}$$

Acknowledgements

The authors are grateful to Vrushali Bokil for helpful comments and suggestions related to perfectly matched layers and to Dr. Vesa Ruuska for helping with calculations in Appendix.

References

[1] I. BABUŠKA, F. IHLENBURG, E. T. PAIK, AND S. A. SAUTER, *A generalized finite element method for solving the Helmholtz equation in two dimensions with minimal pollution*, Comput. Methods Appl. Mech. Engrg., 128 (1995), pp. 325–359.

[2] A. BAMBERGER, P. JOLY, AND J. E. ROBERTS, *Second-order absorbing boundary conditions for the wave equation: a solution for the corner problem*, SIAM J. Numer. Anal., 27 (1990), pp. 323–352.

[3] A. BANEGAS, *Fast Poisson solvers for problems with sparsity*, Math. Comp., 32 (1978), pp. 441–446.

[4] J.-P. BÉRENGER, *A perfectly matched layer for the absorption of electromagnetic waves*, J. Comput. Phys., 114 (1994), pp. 185–200.

[5] ——, *Three-dimensional perfectly matched layer for the absorption of electromagnetic waves*, J. Comput. Phys., 127 (1996), pp. 363–379.

[6] B. L. BUZBEE, F. W. DORR, J. A. GEORGE, AND G. H. GOLUB, *The direct solution of the discrete Poisson equation on irregular regions*, SIAM J. Numer. Anal., 8 (1971), pp. 722–736.

[7] F. COLLINO AND P. MONK, *Optimizing the perfectly matched layer*, Comput. Methods Appl. Mech. Engrg., 164 (1998), pp. 157–171.

[8] ——, *The perfectly matched layer in curvilinear coordinates*, SIAM J. Sci. Comput., 19 (1998), pp. 2061–2090.

[9] B. ENGQUIST AND A. MAJDA, *Absorbing boundary conditions for the numerical simulation of waves,* Math. Comp., 31 (1977), pp. 629–651.

[10] O. G. ERNST, *A finite-element capacitance matrix method for exterior Helmholtz problems*, Numer. Math., 75 (1996), pp. 175–204.

[11] K. GERDES, *A summary of infinite element formulations for exterior Helmholtz problems*, Comput. Methods Appl. Mech. Engrg., 164 (1998), pp. 95–105. Exterior problems of wave propagation (Boulder, CO, 1997; San Francisco, CA, 1997).

[12] K. GERDES AND F. IHLENBURG, *On the pollution effect in FE solutions of the 3D-Helmholtz equation*, Comput. Methods Appl. Mech. Engrg., 170 (1999), pp. 155–172.

[13] D. GIVOLI, *Nonreflecting boundary conditions,* J. Comput. Phys., 94 (1991), pp. 1–29.

[14] I. HARARI, M. SLAVUTIN, AND E. TURKEL, *Analytical and numerical studies of a finite element PML for the Helmholtz equation*, J. Comput. Acoust., 8 (2000), pp. 121–137. Finite elements for wave problems (Trieste, 1999).

[15] E. HEIKKOLA, Y. A. KUZNETSOV, AND K. N. LIPNIKOV, *Fictitious domain methods for the numerical solution of three-dimensional acoustic scattering problems*, J. Comput. Acoust., 7 (1999), pp. 161–183.

[16] E. HEIKKOLA, Y. A. KUZNETSOV, P. NEITTAANMÄKI, AND J. TOIVANEN, *Fictitious domain methods for the numerical solution of two-dimensional scattering problems,* J. Comput. Phys., 145 (1998), pp. 89–109.

[17] E. HEIKKOLA, T. ROSSI, AND J. TOIVANEN, *A parallel fictitious domain method for the three-dimensional Helmholtz equation*, Tech. Rep. B9, Department of Mathematical Information Technology, University of Jyväskylä, Jyväskylä, Finland, 2000. Submitted.

[18] F. Q. HU, *On absorbing boundary conditions for linearized Euler equations by a perfectly matched layer,* J. Comput. Phys., 129 (1996), pp. 201–219.

[19] F. IHLENBURG, *Finite element analysis of acoustic scattering*, Springer-Verlag, New York, 1998.

[20] J. B. KELLER AND D. GIVOLI, *Exact nonreflecting boundary conditions*, J. Comput. Phys., 82 (1989), pp. 172–192.

[21] Y. A. KUZNETSOV, *Computational methods in subspaces*, in Computational processes and systems, No. 2, “Nauka”, Moscow, 1985, pp. 265–350.

[22] Y. A. KUZNETSOV AND A. M. MATSOKIN, *Partial solution of systems of linear algebraic equations*, in Numerical methods in linear algebra (Proc. Third Sem. Methods of Numer. Appl. Math., Novosibirsk, 1978) (Russian), Akad. Nauk SSSR Sibirsk. Otdel. Vychisl. Tsentr, Novosibirsk, 1978, pp. 62–89.

[23] M. LASSAS AND E. SOMERSALO, *Analysis of the PML equations in general convex geometry*, Proc. Roy. Soc. Edinburgh Sect. A, 131 (2001), pp. 1183–1207.

[24] R. C. MACCAMY AND S. P. MARIN, *A finite element method for exterior interface problems*, Internat. J. Math. Math. Sci., 3 (1980), pp. 311–350.

[25] Q. QI AND T. L. GEERS, *Evaluation of the perfectly matched layer for computational acoustics*, J. Comput. Phys., 139 (1998), pp. 166–183.

[26] T. ROSSI AND J. TOIVANEN, *A nonstandard cyclic reduction method, its variants and stability*, SIAM J. Matrix Anal. Appl., 20 (1999), pp. 628–645.

[27] ——, *A parallel fast direct solver for block tridiagonal systems with separable matrices of arbitrary dimension*, SIAM J. Sci. Comput., 20 (1999), pp. 1778–1796.

[28] P. N. SWARZTRAUBER, *The methods of cyclic reduction, Fourier analysis and the FACR algorithm for the discrete solution of Poisson's equation on a rectangle*, SIAM Rev., 19 (1977), pp. 490–501.

[29] E. TURKEL AND A. YEFET, *Absorbing PML boundary layers for wave-like equations*, Appl. Numer. Math., 27 (1998), pp. 533–557.

[30] P. S. VASSILEVSKI, *Fast algorithm for solving a linear algebraic problem with separable variables*, C. R. Acad. Bulgare Sci., 37 (1984), pp. 305–308.

Reports of the Department of Mathematical Information Technology *Series B. Scientific Computing*

B 17/2000 Kaisa Miettinen, Marko M. Mäkelä, Jari Toivanen, Comparison of Four Penalty Function-Based Methods in Handling Constraints with Genetic Algorithms

B 1/2001 Marko M. Mäkelä, Optimality Conditions for Generalized Convex Nonsmooth Optimization

B 2/2001 Perttu Auvinen, Marko M. Mäkelä, Janne Mäkinen, Structural Optimization of Forest Machines – An Analytical Approach

B 3/2001 Perttu Auvinen, Nickolai Banichuk, Marko M. Mäkelä, Janne Mäkinen, Pekka Neittaanmäki, Vasili Saurin, Efficiency Analysis of Crane Systems Optimization

B 4/2001 Perttu Auvinen, Nickolai Banichuk, Marko M. Mäkelä, Pekka Neittaanmäki, Vasili Saurin, Optimal Structural Design Using Discrete Set of Materials

B 5/2001 Marko M. Mäkelä, Review of Bundle Methods for Nondifferentiable Optimization

B 6/2001 Eugenia M. Furems, Oleg I. Larichev, Alexander V. Lotov, Kaisa Miettinen, Grigori V. Roizenson, Psychological Experiments with Individually Difficult Tasks in Discrete MCDM

B 7/2001 Janne V. Kujala, Tuomas J. Lukka, Exact Limiting Solutions for Certain Deterministic Traffic Rules

B 8/2001 Kaisa Miettinen, Marko M. Mäkelä, Classification and Reference Point Based Scalarizing Functions in Multiobjective Optimization

B 9/2001 Anne Setämaa, A Survey of Combinatorial Optimization

B 10/2001 Jari P. Hämäläinen, Kaisa Miettinen, Pasi Tarvainen, Jari Toivanen, Solving a Three-Objective Optimization Problem in Paper Machine Headbox Design Using NIMBUS

B 11/2001 Tommi Kärkkäinen, Kirsi Majava, SAC – Semi-Adaptive, Convex Optimization Methodology for Image Restoration

B 12/2001 Valery E. Grikurov, Erkki Heikkola, Pekka Neittaanmäki, Boris A. Plamenevskii, On Computation of Scattering Matrices and on Surface Waves for Diffraction Gratings

B 13/2001 Kaisa Miettinen, Marko M. Mäkelä, Characterizations of Generalized Trade-Off Directions in Nonconvex Multiobjective Optimization

B 1/2002 Erkki Heikkola, Tuomo Rossi, Jari Toivanen, Fast Direct Solution of the Helmholtz Equation with a Perfectly Matched Layer/an Absorbing Boundary Condition

ISBN 951-39-1150-0
ISSN 1456-436X